Biochimica et Biophysica Acta 1824 (2012) 1382–1393

Contents lists available at SciVerse ScienceDirect

Biochimica et Biophysica Acta

journal homepage: www.elsevier.com/locate/bbapap

Profound conformational changes of PED/PEA-15 in ERK2 complex revealed by NMR backbone dynamics

Edward C. Twomey [a], Dana F. Cordasco [a], Yufeng Wei [a,b,*]

[a] Department of Chemistry and Biochemistry, Seton Hall University, South Orange, NJ 07079, USA
[b] Spectroscopy Resource Center, The Rockefeller University, New York, NY 10065, USA

ARTICLE INFO

Article history:
Received 9 January 2012
Received in revised form 30 May 2012
Accepted 5 July 2012
Available online 20 July 2012

Keywords:
NMR dynamics
PED/PEA-15
ERK2
MAP kinase
Death effector domain

ABSTRACT

PED/PEA-15 is a small, non-catalytic, DED containing protein that is widely expressed in different tissues and highly conserved among mammals. PED/PEA-15 has been found to interact with several protein targets in various pathways, including FADD and procaspase-8 (apoptosis), ERK1/2 (cell cycle entry), and PLD1/2 (diabetes). In this research, we have studied the PED/PEA-15 in a complex with ERK2, a MAP kinase, using NMR spectroscopic techniques. MAP Kinase signaling pathways are involved in the regulation of many cellular functions, including cell proliferation, differentiation, apoptosis and survival. ERK1/2 are activated by a variety of external stimuli, including growth factors, hormones and neurotransmitters. Inactivated ERK2 is primarily found in the cytosol. Once the ERK/MAPK cascade is initiated, ERK2 is phosphorylated and stimulated, allowing it to redistribute in the cell nucleus and act as a transcription factor. Previous studies have shown that PED/PEA-15 complexes with ERK2 in the cytoplasm and prevents redistribution into the nucleus. Although the NMR structure and dynamics of PED/PEA-15 in the free form have been documented recently, no detailed structural and dynamic information for the ERK2-bound form is available. Here we report NMR chemical shift perturbation and backbone dynamic studies at the fast ps–ns timescale of PED/PEA-15, in its free form and in the complex with ERK2. These analyses characterize motions and conformational changes involved in ERK2 recognition and binding that orchestrate the reorganization of the DED and immobilization of the C-terminal tail. A new induced fit binding model for PED/PEA-15 is proposed.

1. Introduction

PED/PEA-15 (phosphoprotein enriched in diabetes/phosphoprotein enriched in astrocytes, 15 kDa) is a small 130-residue cytosolic protein that is ubiquitously expressed in different human tissues and highly conserved among mammals [1,2]. It consists of an N-terminal death-effector domain (DED) and a C-terminal tail with irregular structure [3]. The DEDs, together with the structurally related death domain (DD), caspase recruitment domain (CARD) and pyrin domain (PYD), are members of the death motif super family characterized by a conserved six α-helix bundle structure [4]. PED/PEA-15 interacts with a diverse array of proteins with and without DEDs [3], and its binding specificity is mediated by the phosphorylation on two serine residues on the C-terminal tail [5,6], S104, the substrate for protein kinase C (PKC), and S116, phosphorylated by calcium/calmodulin-dependent protein kinase II (CamKII) or protein kinase B/Akt [2,7,8]. The N-terminal DED of PED/PEA-15 can interact with other DED-containing proteins, including Fas-associated protein with death domain (FADD), FADD-like IL-1β-converting enzyme (FLICE), and procaspase-8 [9], and it can be recruited to the death-inducing signaling complex (DISC) [10], playing an antagonistic role in death signaling mediated by members of the tumor necrosis factor (TNF) receptor super family [11].

PED/PEA-15 can also restrain cellular proliferation by regulating the mitogen-activated protein (MAP) kinase signaling pathway through binding to extracellular regulated kinase 1 and 2 (ERK1/2), preventing translocation of ERK1/2 into the nucleus, and blocking ERK-dependent cell proliferation and migration [12,13]. In addition, PED/PEA-15 is overexpressed in adipose and skeletal muscle tissues and in skin fibroblasts from type 2 diabetic individuals independent of obesity, causing resistance to insulin action in glucose uptake [14]. PED/PEA-15 interacts with phospholipase D (PLD) isoforms 1 and 2, elevating intracellular levels of diacylglycerol (DAG), thereby activating diacylglycerol-sensitive PKCα isoform [15]. Activation of PKCα in PED/PEA-15 overexpressing cells and tissues prevents

Abbreviations: PED/PEA-15, phosphoprotein enriched in diabetes/phosphoprotein enriched in astrocytes, 15 kDa; ERK, extracellular regulated kinase; DED, death effector domain; CSP, chemical shift perturbation; TROSY, transverse relaxation optimized spectroscopy

* Corresponding author at: Department of Chemistry and Biochemistry, Seton Hall University, South Orange, NJ 07079, USA. Tel.: +1 973 275 2335; fax: +1 973 761 9772.
E-mail address: Yufeng.Wei@shu.edu (Y. Wei).

1570-9639/$ – see front matter © 2012 Elsevier B.V. All rights reserved.
doi:10.1016/j.bbapap.2012.07.001

insulin induction of the PKCζ isoform, which is the major activator of glucose transporter 4 (GLUT4) [16,17].

MAPK pathways are involved in the regulation of many diverse cellular functions, including cell proliferation, differentiation, apoptosis and survival [18]. The MAPK pathway is highly regulated by protein–protein interactions, which makes it an intriguing therapeutic target. Dysregulation of MAPK pathways is indicated in a variety of diseases, including diabetes and cancer. Extracellular regulated kinase 1 and 2 (ERK1/2) are two kinases controlled by the mitogen-activated protein kinase (MAPK) signaling cascade, and are activated by a range of agonists including growth factors, hormones, and neurotransmitters. When activated, ERK1/2 can translocate into the nucleus and serve as transcription factors, regulating a wide variety of cell functions, including cell differentiation, apoptosis, proliferation, and maintenance of homeostasis [18,19]. ERK 1 (43 kDa) and ERK 2 (41 kDa) are approximately 83% identical and both are activated by dual phosphorylation on Thr and Tyr residues [18,20]. The ERK activation cascade is initiated by extracellular agonists that activate the GTPase, Ras. Ras then activates the phosphorylation cascade, beginning with Raf, which exists in three isomeric forms: A-Raf, B-Raf, and C-Raf. The activated Raf phosphorylates MEK (mitogen extracellular-regulated kinase) at serine and threonine residues, which subsequently phosphorylates ERK1/2. The activation of ERK1/2 stimulates the ERK molecules to translocate into the nucleus and regulate a variety of cellular functions.

PED/PEA-15 plays a crucial regulatory role in the ERK/MAP kinase pathway, and is directly involved in oncogenesis. Recent literature suggests that, due to its anti-apoptotic feature, PED/PEA-15 overexpression is associated with the development of human tumors [10,21–24], can support tumor cell survival, and may mediate resistance to chemotherapy [24]. In addition, PED/PEA-15 protects tumor cells from glucose deprivation-induced apoptosis by regulating ERK activity in glioblastoma that is required for up-regulation of glucose transporter 3 [4]. Other evidence suggests that, particularly in tumors driven by oncogenic *Ras*, PED/PEA-15 induced cytosolic localization of ERK1/2 prevents oncogenic transformation and leads to cellular senescence [25], suppressing tumor cell proliferation and migration in breast cancer and ovarian cancer through induced autophagy [26–29]. While the anti-apoptotic and oncogenic function of PED/PEA-15 is well documented, PED/PEA-15 may contribute to the inhibition of tumor cell invasion, and is associated with prolonged overall survival among cancer patients.

The structure of PED/PEA-15 was solved previously from solution NMR [30], and an NMR backbone dynamics study was recently reported in the free-form [31]. The interactions between PED/PEA-15 and ERK2 have been examined using a fluorescence binding assay, which reported that PED/PEA-15 binds to ERK2 to a high affinity, with a $K_d = 133 \pm 5$ nM, and phosphorylation states on both PED/PEA-15 and ERK2 do not significantly affect the stability of the complex [13,32]. A recent light scattering study demonstrated that PED/PEA-15 and ERK2 form a strong 1:1 complex of ~57 kDa [33]. Here we have studied the dynamic properties of PED/PEA-15 in its ERK2 complex using high resolution NMR spectroscopy. While our chemical shift perturbation (CSP) and dynamic data in the ERK2-bound PED/PEA-15 confirmed the essential roles of the C-terminal tail, especially the putative pseudo D-site sequence at the end of the tail [13,30], our data suggested an alternative binding model to the previously proposed binding interface on the DED that involves the α1–α2 and α5–α6 loops, including an essential residue, D74 [30]. Based on our data reported here, we propose a novel binding model that upon recognition of the pseudo D-site sequence on the PED/PEA-15 C-terminal tail by the ERK2 D-recruitment site, the PED/PEA-15 DED undergoes significant conformational change, associated with rearrangement of vital polar interaction sites (hydrogen bonding and charge–charge interactions) on the protein surface to create an induced binding interface to ERK2. In this induced-fit binding model, the key residue D74 acts as a hinge to facilitate the rearrangement of the charged and polar interactions on PED/PEA-15 upon ERK2 binding. However, contrary to the model suggested from the mutagenesis study, D74 is not directly involved in contact with ERK2 protein.

2. Methods and materials

2.1. Protein expression and purification

Full length PED/PEA-15 protein was expressed and purified as described previously [30]. Briefly, the protein was cloned into a pQE-9 vector (Qiagen), and was expressed as hexahistidine (His_6) tagged protein at the N-terminus. Uniformly $^2H/^{15}N$ and $^2H/^{13}C/^{15}N$ labeled protein was overexpressed in *Escherichia coli* BL21 cells in minimal medium in D_2O containing $^{15}NH_4Cl$ and/or ^{13}C-glucose as the sole nitrogen and carbon sources, respectively. Cells were grown at 37 °C to an optical density O.D.600 ~ 0.4–0.7 and then induced with 1 mM isopropyl-β-D-thiogalactopyranoside (IPTG) for 4 h. The cells were suspended in 50 mM Tris buffer pH 8.0, 1 M NaCl, 30 mM imidazole and 10 mM benzamidine hydrochloride, lysed with a French press, and centrifuged. The protein was isolated by Ni^{2+} affinity chromatography and subsequently purified to homogeneity by anion-exchange chromatography (MonoQ HR 16/10).

2.2. NMR spectroscopy

The free PED/PEA-15 NMR sample was prepared at 0.7 mM protein in 10 mM sodium phosphate buffer pH 7.0, 1 mM dithiothreitol (DTT) and 50 μM NaN_3 in 90%/10% H_2O/D_2O. The PED/PEA-15/ERK2 complex was formed using the uniformly labeled PED/PEA-15 with unphosphorylated ERK2 that was expressed and purified as described [34]. The complex NMR sample was prepared with 0.7 mM uniformly labeled PED/PEA-15 and a stoichiometric amount of ERK2 (1:1 molar equivalent) in 10 mM sodium phosphate buffer pH 7.0, 150 mM NaCl, 1 mM DTT and 50 μM NaN_3 in 90%/10% H_2O/D_2O.

All NMR experiments were acquired at 25 °C on a Bruker Avance 800 MHz NMR spectrometer, operating at ^1H frequency of 800.35 MHz, and ^{15}N frequency of 81.1 MHz, equipped with triple-resonance cryoprobes at the New York Structural Biology Center (NYSBC). 2D ^1H–^{15}N correlation experiments for free PED/PEA-15 and PED/PEA-15/ERK complexes at 1:0.5, 1:1, and 1:2 ratios were obtained using TROSY techniques [35,36]. TROSY-based protein backbone dynamics experiments [37] were performed to measure ^{15}N R_1, ^{15}N R_2, and [^1H]–^{15}N heteronuclear NOE for both free PEA-15 and PEA-15/ERK2 complex at a 1:1 ratio. Typically, 7 time points were collected for R_1 and R_2 experiments, and each set included one duplicate measurement to allow an estimation of uncertainty. The delay times were 65, 150, 246, 363, 523, 758, and 1142 ms for R_1 experiments, and 20.8, 41.5, 62.2, 82.9, 145.0, 186.4, and 227.8 ms for R_2 experiments. All NMR data were processed using NMRPipe [38] and analyzed using NMRViewJ [39]. Peak intensities were measured for the calculation of the relaxation times and heteronuclear [^1H]–^{15}N NOE values. R_1 and R_2 rates were determined by fitting peak intensities (I) at multiple relaxation delays (t) to the equation $I(t) = I_0 e^{-R_i t}$ using the graphing program IGOR Pro (www.wavemetrics.com). Uncertainties in R_1 and R_2 represent the statistical errors obtained from the fitting procedures. Steady-state heteronuclear [^1H]–^{15}N NOEs were calculated as the ratio of ^1H–^{15}N correlation peak heights in the spectra acquired with and without ^1H saturation and their uncertainties were set to 5%.

2.3. Relaxation data analysis

The ^{15}N R_1, R_2, and [^1H]–^{15}N heteronuclear NOE data were further analyzed using the suite of *Mathematica* notebooks for protein main

chain relaxation data analysis [40]. The overall diffusion tensor was determined using the corresponding notebook from residues with NOE > 0.7 in the DED domain. The per residue plots of $J(0)$, $J(\omega_N)$, and $J(0.87\omega_H)$ were generated from reduced spectral density mapping using the equation described by Farrow et al. [41,42], and implemented in the *Mathematica* notebook. The per residue correlation time was calculated from $J(0)$ and $J(\omega_N)$ spectral densities using equation described by Viles et al. [43]. The distributions of spectral densities and correlation times were performed using in-house scripts written for Igor Pro graphing software. Model free analysis was attempted using the *Mathematica* notebook [40], ModelFree 4.20 [44,45], Fast-ModelFree [46], and TENSOR2 [47]. The S^2 order parameters were also estimated from $J(0)$ and $J(\omega_N)$ spectral densities using the equation described by Viles et al. [43].

3. Results

3.1. Chemical shift perturbation

The TROSY ^1H–^{15}N correlation experiments were performed on the perdeuterated PED/PEA-15 and its ERK2 complexes at 1:0.5, 1:1, and 1:2 ratios. A number of PED/PEA-15 resonances experience significant spectral shifts upon association with ERK2, as shown in the superposition of the TROSY ^1H–^{15}N correlation spectra of PED/PEA-15 in the free-state and the 1:1 complex of ERK2-bound state (Fig. 1A). At higher ERK2 ratios, however, no spectral changes can be observed, consistent with a tight 1:1 complex formed between PED/PEA-15 and ERK2 as indicated in the fluorescence anisotropy assay [13] and the light scattering studies [33] (for details on the

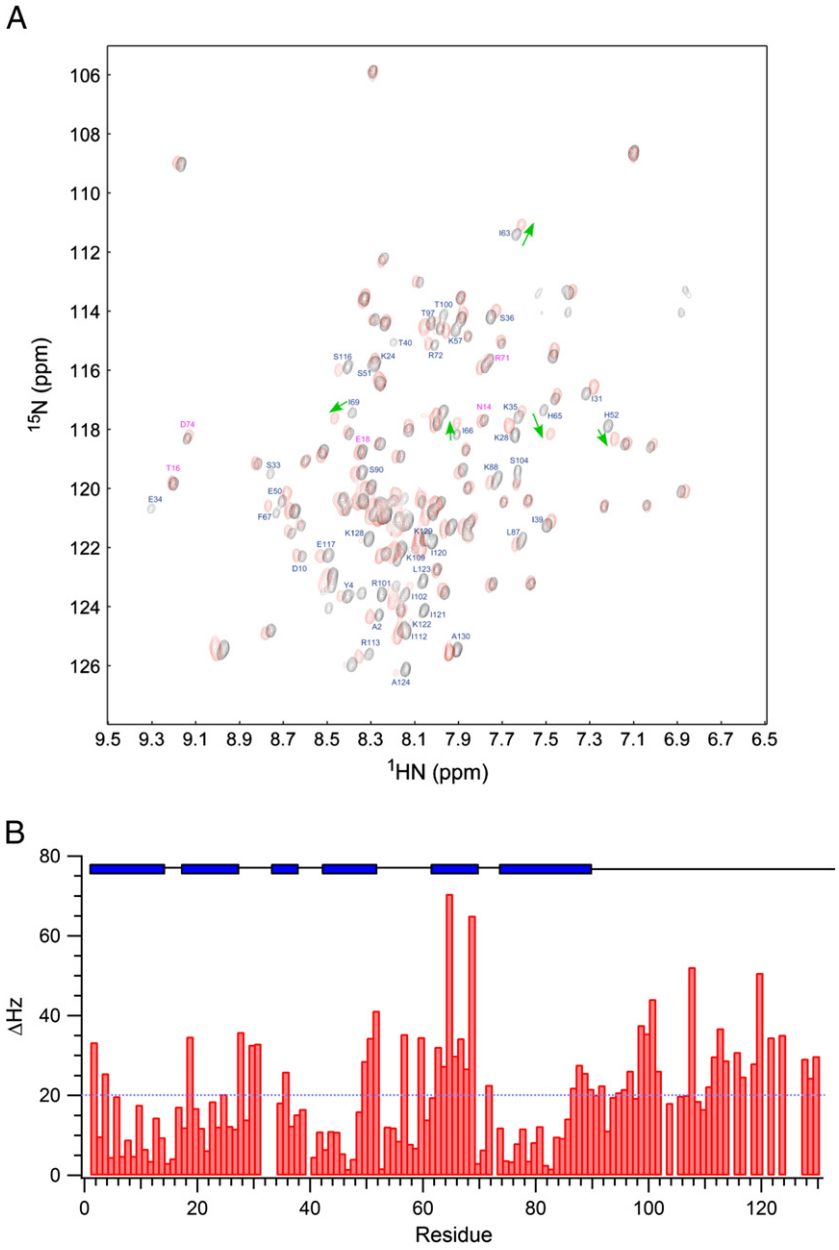

Fig. 1. (A) Superposition of the ^1H–^{15}N TROSY spectra of PED/PEA-15 in the free (black) and ERK2-bound form (red) at 1:1 ratio. Resonances that display significant changes in chemical shifts in the presence of ERK2 are labeled in blue and indicated by green arrows. Peaks for residues found to be important in ERK2 binding are labeled in magenta. (B) Chemical shift perturbation (CSP), defined as $\Delta Hz = \left[(\Delta H/Hz)^2 + (\Delta N/Hz)^2\right]^{1/2}$, is displayed against residue number. The positions of α-helices of PED/PEA-15 are represented as blue bars on top of the figure.

NMR titration experiments, please refer to the Supplementary materials). Residues experiencing significant shifts (>20 Hz) or broadening are indicated in the figure. Chemical shift perturbation (CSP), defined as $\Delta Hz = \left[(\Delta H/Hz)^2 + (\Delta N/Hz)^2\right]^{1/2}$ displays the most pronounced shifts for residues E50, S51, and H52 in the α4 helix, and residues I63, H65, I66, and I69 in the α5 helix of the folded DED domain (Fig. 1B), although these two helices have not been shown to be essential in ERK2 binding [30]. Therefore, significant conformational change in the α4 and α5 helices is implicated in the ERK2 complex. Interestingly, the CSP feature for these residues is consistent with relaxation behavior, exhibiting large fluctuations in dynamics in this region, indicative of increased motion upon ERK binding (see below). On the other hand, the residues that were reported to be essential for binding ERK2 by the mutagenesis study [30], including residues N14, T16, and E18 in between α1 and α2, and R71 and D74 in between α5 and α6, only display moderate CSP. In fact, the original NMR study of the PED/PEA-15 binding with ERK2 showed that the resonances of these essential residues were all broadened rather than shifted upon interacting with ERK2 [30].

Another region that displays large CSP values is in the C-terminal tail, which has been shown to be important in binding ERK2. The large CSP values are observed in residues E92, D96, Y108, K109, E119, I120, I121, and K128. It has been speculated that the PEA-15 sequence ^{121}IKLAPPPKK^{129} binds to the ERK2 D-recruitment site (DRS, also called DEJL-domain), reminiscent of the consensus binding sequence $(R/K)_{2-3}X_{4-6}\phi_A X\phi_B$ to the DRS of ERK2 in the *reverse* direction, where ϕ_A and ϕ_B are hydrophobic residues (I, L, or V), and X represents any amino acid [13,32]. The essential residues (I121, L123, K128, and K129) for the putative binding of ERK2 DRS do show significant shifts upon complex formation.

3.2. Relaxation parameters

Recently, the backbone dynamics of PED/PEA-15 in the free-state has been reported, and interesting dynamic features have been observed in correlation to the protein functional sites [31]. We studied the backbone dynamics of ^{2}H,^{15}N-labeled PED/PEA-15 in the ERK2-bound state, and quantitative ^{15}N relaxation parameters were obtained using TROSY techniques at 800 MHz field strength (Fig. 2) [37]. As a comparison, we also measured the relaxation data of the ^{2}H, ^{15}N-labeled PED/PEA-15 in its free-state at the same field strength and TROSY-based sequences. The measured R_1 values for the free PED/PEA-15 are, in general, larger than the reported values, due to the fact that we were using a perdeuterated protein. The general trends for R_1, however, are in good agreement with the literature. The R_2 and [^{1}H]–^{15}N heteronuclear NOE also agree with the reported values. In particular, the average relaxation values are $R_1 = 2.44 \pm 0.44\ s^{-1}$, $R_2 = 12.5 \pm 2.5\ s^{-1}$, $R_2/R_1 = 5.23 \pm 1.38$, and NOE = 0.77 ± 0.28 for the DED (residues 1–90); and $R_1 = 2.99 \pm 0.79\ s^{-1}$, $R_2 = 4.7 \pm 2.3\ s^{-1}$, $R_2/R_1 = 1.66 \pm 1.01$, and NOE = −0.50 ± 0.58 for the C-terminal tail (residues 91–130). The C-terminal tail residues have generally higher R_1 values than the DED residues, possibly due to nanosecond motions, but show lower R_2 values than DED residues, indicative of higher degree of structural disorder, which is consistent with low NOE values.

The ERK2-bound PED/PEA-15 displays significant variation from the free-state PEA-15. On average, the relaxation values are $R_1 = 2.99 \pm 0.60\ s^{-1}$, $R_2 = 27.6 \pm 6.8\ s^{-1}$, $R_2/R_1 = 9.62 \pm 3.03$, and NOE = 0.68 ± 0.27 for the DED; and $R_1 = 3.20 \pm 0.75\ s^{-1}$, $R_2 = 15.3 \pm 5.4\ s^{-1}$, $R_2/R_1 = 4.78 \pm 1.73$, and NOE = −0.23 ± 0.60 for the C-terminal tail. The R_1 values are more consistent throughout the DED and the C-terminal tail, indicating a restrained nanosecond motion in the tail upon binding to ERK2. However, residues between 61 and 88, corresponding to helices 5–6, display consistently elevated R_1 values comparing to the free form in the same segment, indicating that these residues exhibit higher nanosecond motions upon binding ERK2. The substantial increase in the R_2 values is consistent with the reduced overall tumbling rate upon complex formation. The heteronuclear NOE values indicate a slightly flexible DED but a more rigid tail comparing to the free-state PED/PEA-15. S104 in the tail exhibits one of the lowest R_1, R_2, and NOE values in the ERK2-bound state, whereas D110 displays high R_1, R_2, and NOE values. In addition, extraordinarily low NOE values are observed for the DED residues E64 and E68 in the middle of helix α5, and R72, part of the charge triad, in the α5–α6 loop. This region also displays the largest chemical shift perturbation, indicating a significant conformational change upon binding. However, the residues in this region are not crucial for ERK2 binding based on the mutagenesis study [30]. This region, therefore, might act as a scaffold to facilitate recognition of ERK2. Residues T16, D19 (part of charge triad), and L20 of α2, and residues K35, I39, and T41 of α3–α4 loop also display lowered NOE values than the free form. Lowered NOE values for residues D74 (part of charge triad), L75, and L76 are also observed, but to a lesser extent.

3.3. Rotational diffusion tensor

The isotropic global correlation time for the free-form PED/PEA-15 was estimated from R_2/R_1 ratio of 69 residues within the DED with heteronuclear NOE > 0.7 and coordinates from the NMR structure of PEA-15 (PDB ID: 1N3K) [30], yielding a value of $\tau_m = 8.13$ ns with $\chi^2 = 199$. This value is consistent with the expected value for a 130-residue protein, and in good agreement with the reported overall correlation time reported previously [31]. The diffusion model for PEA-15 protein is best described as axially symmetric, and the tensor parameters were estimated as $D = 2.31 \times 10^7$, $D = 1.60 \times 10^7$, $\phi = 82.8°$, and $\theta = 0.80°$, with $\chi^2 = 140$. The value for an axially symmetric diffusion tensor is $\tau_c = 8.04$ ns.

For the ERK2-bound PED/PEA-15 protein, the isotropic global correlation time was estimated from R_2/R_1 ratio of 42 residues within the DED with heteronuclear NOE > 0.7, giving a value of $\tau_m = 11.57$ ns with $\chi^2 = 65.9$. The axially symmetric diffusion tensor analysis yields $D = 1.55 \times 10^7\ s^{-1}$, $D = 1.05 \times 10^7\ s^{-1}$, $\phi = 70.8°$, and $\theta = 30.5°$, with $\chi^2 = 51.6$. These parameters are also summarized in Table 1. The reduced axially symmetric diffusion tensor values and higher global correlation time indicate the formation of a larger complex. However, this global correlation time of 11.57 ns is considerably small comparing to the expected value for a 57 kDa complex. A per-residue correlation time analysis shows that while the majority of the PED/PEA-15 residues have correlation times, τ_c, centered around this global τ_m, a number of residues on helices α1, α5, and α6 possess higher τ_c values around 15 ns, consistent with the 57 kDa complex (see text below).

3.4. Reduced spectral density mapping

Reduced spectral density mapping is a convenient method to characterize the motion of each ^{1}H–^{15}N bond vector at 0, ^{15}N, and ^{1}H frequencies without knowing the nature of molecular global rotational diffusion [41,48]. The $J(0)$ spectral density function is equal to $\frac{2}{5}\tau_m$, where τ_m is the rotational correlation time, in the absence of internal motions. A $J(0)$ value less than $\frac{2}{5}\tau_m$ is indicative of subnanosecond flexibility of the N–H bond vector. An elevated $J(0)$ spectral density ($> \frac{2}{5}\tau_m$) indicates slow micro- to millisecond motions, or R_{ex}. The $J(\omega_N)$ and $J(0.87\omega_H)$ spectral densities, on the other hand, are not affected by the slow R_{ex} motions, and thereby can be used to isolate the slow motions observed in the $J(0)$ spectral densities. Higher than average $J(0.87\omega_H)$ spectral densities also indicate enhanced mobility in the fast pico- to nanosecond timescale. In addition, $J(0)$ spectral density is dominant in the transverse ^{15}N relaxation rate, R_2, and $J(\omega_N)$ is the major contributor to the longitudinal ^{15}N relaxation rate, R_1, while $J(0.87\omega_H)$ is directly proportional to the cross-relaxation

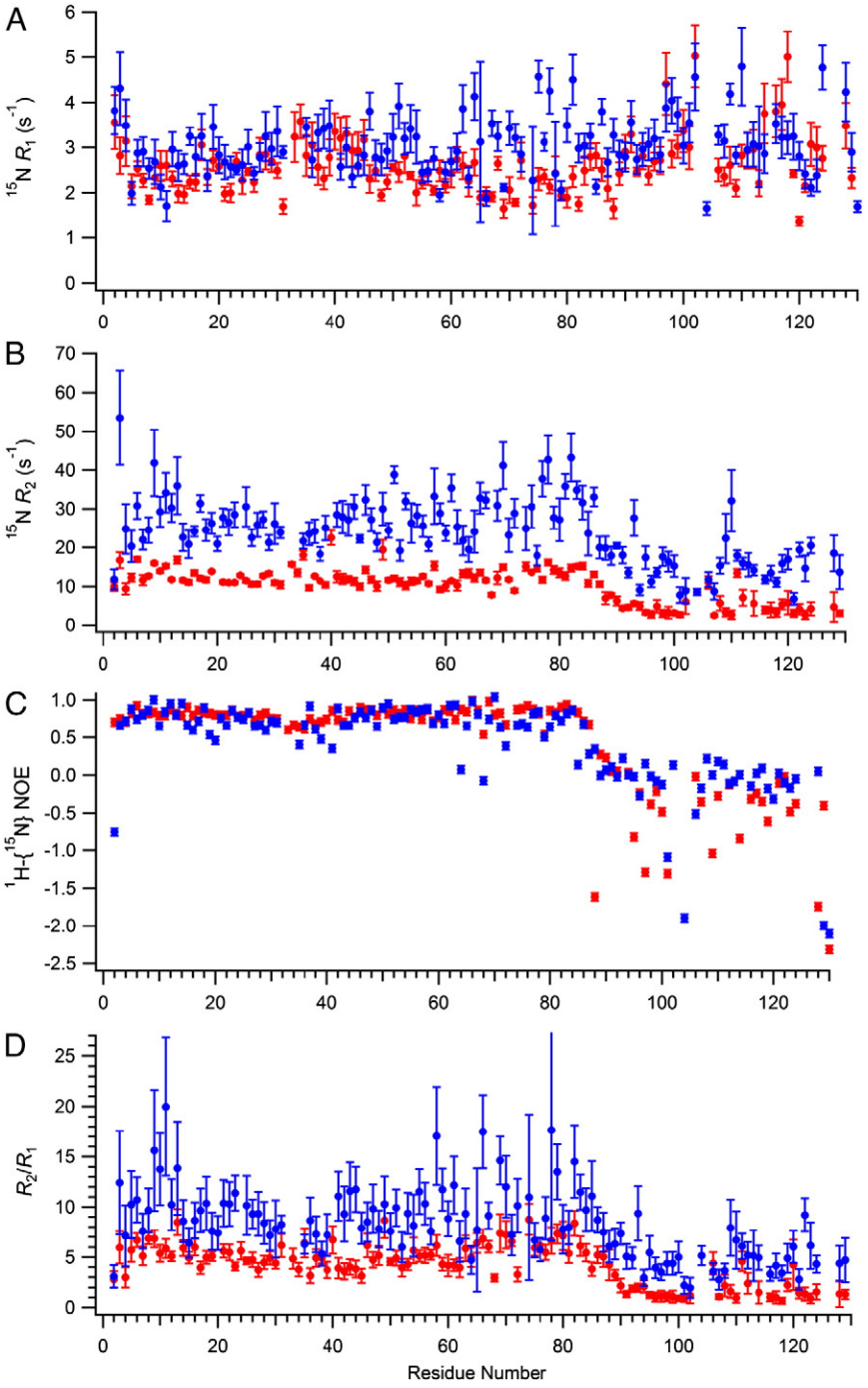

Fig. 2. Relaxation rates $R_1 = 1/T_1$ and $R_2 = 1/T_2$, heteronuclear [^{1}H]–^{15}N NOE, and R_2/R_1 values for PED/PEA-15 in the free (red) and ERK2-bound form (blue).

rate constant, $R_{H\rightarrow N}$. As a result, the spectral densities are consistent with the primary experimental relaxation rates.

The reduced spectral density functions at $J(0)$, $J(\omega_N)$, and $J(0.87\omega_H)$ frequencies were calculated for each residue of PEA-15 in both free- and ERK2-bound forms, and are plotted in Fig. 3. PEA-15 protein in the complex has $J(0)$ spectral densities consistently higher than the values in the free form due to the increased R_2 rate upon complex formation. The average $J(0) = 4.23 \pm 1.00$ ns for the DED is in agreement with $\frac{2}{5}\tau_m = 3.25$ ns. The significantly reduced $J(0) = 0.90 \pm 0.70$ ns spectral density indicates a highly flexible C-terminal tail in sub-nanosecond timescale. There is only one residue, E68, in the DED which has a $J(0)$ spectral density smaller than one standard deviation, indicative of increased mobility in the fast timescale. However, residues E3, T6, Q9, L11, and N13 in α1, S33, K35 in α3, T40 and L49 in α4, D58 in loop α4–α5, and S70, D74, M78, Y82, R83, and T84 in α6, all exhibit $J(0)$ spectral densities higher than one standard deviation, with the highest $J(0)$ values observed in K35 (6.29 ns/rad), T40 (7.89 ns/rad), and L49 (6.93 ns/rad), reflecting enhanced slow micro- to millisecond R_{ex} motions in these residues. Notably, most of these residues are charged or polar residues on the protein surface, with D74 critical in ERK2 binding.

The ERK2-bound PED/PEA-15 has average $J(0)$ spectral densities of 9.84 ± 2.58 ns for the DED, and 5.05 ± 2.02 ns for the C-terminal tail. The $\frac{2}{5}\tau_m$ is 4.63 ns for the complex, and surprisingly, this value matches the $J(0)$ value of the C-terminal tail, while the DED has an average $J(0)$ spectral density about twice the $\frac{2}{5}\tau_m$ value. Three residues from the

Table 1
Dynamic parameters for PED/PEA-15 in free and ERK2-bound forms.

	Free form		Bound form	
	DED	Tail	DED	Tail
τ_m (ns)	8.13		11.57	
D (s^{-1})	2.31×10^7		1.58×10^7	
D (s^{-1})	1.60×10^7		1.04×10^7	
ϕ (°)	82.8		70.8	
θ (°)	0.80		30.5	
$\tau_{c,i}$ (ns)	7.91 ± 1.22		10.55 ± 1.65 15.13 ± 0.93	
R_2/R_1	5.23 ± 1.38	1.66 ± 1.01	9.62 ± 3.03	4.78 ± 1.73
$J(0)$ ns/rad	4.23 ± 1.00	0.90 ± 0.70	9.84 ± 2.58	5.05 ± 2.02
$J(\omega N)$ ns/rad	0.60 ± 0.11	0.60 ± 0.14	0.71 ± 0.14	0.69 ± 0.18
$J(0.87\omega H)$ ns/rad	0.0090 ± 0.0084	0.070 ± 0.032	0.015 ± 0.015	0.058 ± 0.021

C-terminal tail have $J(0)$ spectral densities outside the high limit of one standard deviation, D93 (9.87 ns/rad), K109 (7.89 ns/rad), and D110 (11.15 ns/rad), representing candidates for slow R_{ex} motions. The $J(0)$ spectral densities for the DED in the complex suggest that the DED relaxation R_2 rate is dominated by R_{ex} throughout the sequence. This result is highly unexpected, and we propose that upon complex formation, the C-terminal tail binds to ERK2 tightly, and moves together as part of the complex, while the DED undergoes coordinated motions accompanying a conformational change, resulting in much higher $J(0)$ spectral densities (see Discussion below). Further, several residues display additional slow timescale R_{ex} motions on top of the whole domain chemical exchange as reflected in $J(0)$ spectral densities outside the high limit of the normal distribution (Fig. 3A), including residues Q9, L11, and N13 in α1, S51 in α4, S61 in α5, and S70, T77, M78, D81, Y82, and R83 in α6, with highest $J(0)$ values observed in S70 (15.0 ns/rad), M78 (15.9 ns/rad), and Y82 (15.8 ns/rad).

The $J(\omega_N)$ values exhibit less variation with residue number for both free-form and ERK2-bound PED/PEA-15 (Fig. 3B). Consistent with the R_1 values, the bound form displays higher $J(\omega_N)$ spectral densities between residues 61 and 88 in helices α5 and α6 than the free form, indicating increased motions at the fast timescale for these residues.

The high-frequency spectral density function $J(0.87\omega_H)$ has much smaller values with an opposite trend from $J(0)$, where larger values reflect increased fast timescale, pico- to nanosecond motions (Fig. 3C), recalling slow R_{ex} motions are not reflected in $J(0.87\omega_H)$ spectral densities. As expected, the $J(0.87\omega_H)$ values for the C-terminal tail (0.070 ± 0.032 ns) are about a magnitude larger than those of the DED (0.0090 ± 0.0084 ns) in the free form. Comparing $J(0.87\omega H)$ spectral densities for the free and ERK2-bound form of the protein, it appears that the C-terminal tail is less flexible in the fast timescale for many residues, as evidenced of $J(0.87\omega H)$ reduced to 0.058 ± 0.021 ns in the bound form, while residues in the DED display enhanced flexibilities with observed increased $J(0.87\omega H)$ to 0.015 ± 0.015 ns. The largest $J(0.87\omega_H)$ values are observed for residues E64 (0.0597 ns/rad) and E68 (0.0545 ns/rad) in α5. Interestingly, residues in α5 also exhibit the largest chemical shift perturbation upon binding to ERK2, although they are not essential in ERK2 binding. Other residues that show increased $J(0.87\omega_H)$ values upon complex formation include I15, T16, L17, D19, and L20 of α2, K35, I39, and T41 around loop α3–α4, R72 on loop α5–α6, and L75 of α6. Many residues in α5 and α6 exhibit both increased $J(0)$ and $J(0.87\omega_H)$ spectral densities when PED/PEA-15 is bound to ERK2, indicating complicated motions in this region across a wide range of time scales (ps–ms).

The 40-residue long, disordered C-terminal tail is also believed to influence the overall tumbling of the globular DED in both free- and ERK2-bound forms. As a result, the motions of the folded DED of PED/PEA-15 cannot be described by a simple anisotropic tumbling model with unique diffusion tensor elements, $D_{\cdot}$ and $D^{\perp}$, and the motions of individual N–H vectors are better characterized by a distribution of correlation times on a nanosecond timescale, reflecting the conformational disorder of the C-terminal tail. This phenomenon has been observed previously [43]. The effective rotational correlation time ($\tau_{c,i}$) for each residue can be calculated from $J(0)$ and $J(\omega_N)$: $\tau_{c,i} = \frac{1}{\omega_N}\left[\frac{J(0)_i - J(\omega_N)_i}{J(\omega_N)_i}\right]^{1/2}$ [49]. The $\tau_{c,i}$ values should be the same assuming isotropic tumbling and the absence of both fast internal motions and slow conformational changes. We have calculated the $\tau_{c,i}$ value for each rigid residue with NOE > 0.7 for PED/PEA-15 in free-form (Fig. 5A). The per-residue correlation times can be characterized by a Gaussian distribution centered at 7.48 ns with a width of 1.71 ns (Fig. 5B). The center of the $\tau_{c,i}$ distribution is consistent with the estimated overall $\tau_m = 8.13$ ns, but the values cover a wide range from 5 ns to above 10 ns.

Surprisingly, binding to ERK2 does not simplify the dynamic behavior of PED/PEA-15. Instead, the globular DED in the ERK2-bound state exhibits overly complicated dynamic features compared to the free-form, as seen in the spectral density functions at all three frequencies. The per-residue correlation times also have a wide range of distribution, from less than 8 ns to about 17 ns, for rigid residues with NOE > 0.7 (Fig. 5A). A fit of $\tau_{c,i}$ for the bound state into a Gaussian distribution yielded a center of 10.55 ns with the width of 1.65 ns (Fig. 5C and Table 1). The fitted center of the distribution is consistent with the overall correlation time τ_m, but a number of residues exhibit longer correlation times, which cannot be readily fitted into the main Gaussian curve but appear as a second distribution centered at 15.1 ± 0.9 ns (Table 1), a tumbling rate more consistent with the size of the complex. These residues include Q9 (14.6 ns), L11 (16.9 ns), N13 (13.9 ns), D58 (15.5 ns), I66 (15.6 ns), I69 (14.4 ns), M78 (15.8 ns), and Y82 (14.3 ns), located in helices α1, α5 and α6. This is an interesting observation in that many residues on PED/PEA-15 have intermediate correlation times in between the free-form (~8 ns) and the complex form (~15 ns), while only a small number of residues experience correlation times of the complex. We hypothesize that the residues with long correlation times (~15 ns) are in tight association with ERK2, and are located at the binding interface of the complex.

4. Discussion

Reduced spectral density functions, $J(0)$, $J(\omega_N)$ and $J(0.87\omega_H)$, derived from relaxation parameters, R_1, R_2, and heteronuclear $[^1H]$–^{15}N NOE, provide complementary information about motions along the polypeptide backbone. The spectral density function at zero frequency reflects both internal motions on the ps–ns timescale that are faster than the overall tumbling of the protein and slow R_{ex} motions on the ms–μs timescale. The high-frequency spectral density function, $J(0.87\omega_H)$, is only sensitive to fast internal motions on ps–ns timescale. Typically, these $J(0)$ and $J(0.87\omega_H)$ functions show opposite trends, as observed in PED/PEA-15 protein where residues in the globular DED, in general, have larger $J(0)$ and smaller $J(0.87\omega_H)$ values compared to C-terminal tail residues because of increased internal flexibility of the structurally disordered C-terminal tail. The $J(\omega_N)$ function is less sensitive to variations in internal motions under the global rotational correlation times for both free-state PED/PEA-15 and the complex formed between ERK2 and PED/PEA-15 proteins, and no significant differences in this function have been observed for the structured DED and the tail.

Detailed analyses of the reduced spectral density mapping revealed that PED/PEA-15 exhibits extremely complicated dynamic behavior in both free- and ERK2-bound forms. In its free form, the highly disordered and flexible C-terminal tail significantly affects the overall tumbling of the protein, resulting in a wide distribution of the correlation times for individual N–H bond vectors in the globular DED (Fig. 4B). Upon complex formation with ERK2, the C-terminal tail of PED/PEA-15

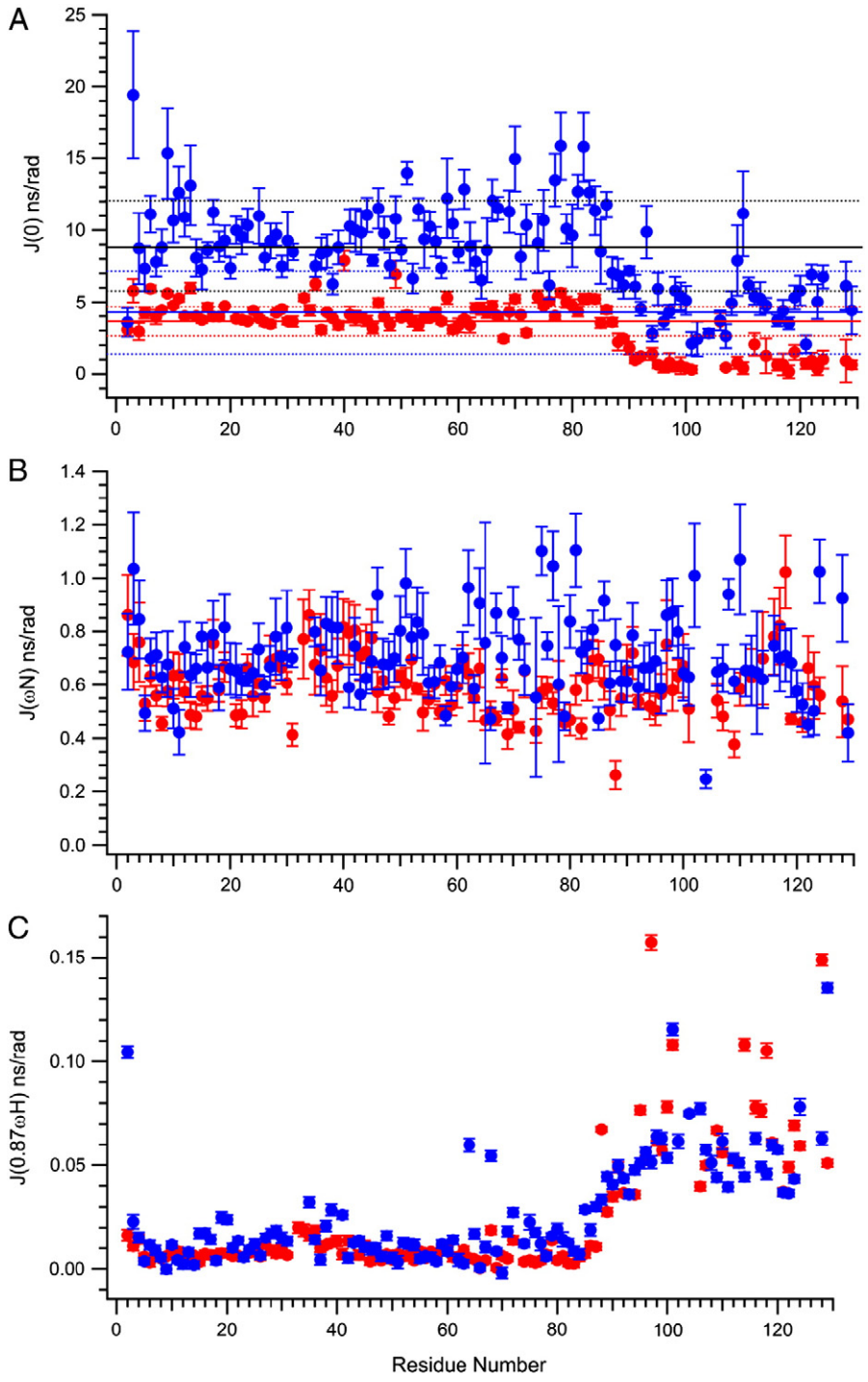

Fig. 3. Reduced spectral density functions (A) $J(0)$, (B) $J(\omega_N)$, and (C) $J(0.87\omega_H)$ for PED/PEA-15 in the free (red) and ERK2-bound form (blue). In the $J(0)$ plot (A), solid red and blue lines represent $\frac{2}{5}\tau_m$ for the free and ERK2-bound forms, respectively; and dashed red and blue lines represent one standard deviation from the mean value of the $J(0)$ spectral densities for the DED of the free form and the tail of the ERK2-bound form, respectively. The solid and dashed black lines represent the mean and one standard deviation, respectively, of the $J(0)$ spectral density for the DED of the ERK2-bound form. See text for detail.

becomes less flexible, while the DED shows an increased complexity in dynamics. The putative ERK2 DRS binding sequence at the C-terminal tail of PED/PEA-15, ^{121}IKLAPPPKK^{129}, which displays large chemical shift perturbations upon complex formation, shows $J(0)$ spectral densities that are within the vicinity of the expected $\frac{2}{5}\tau_m$ value, although the high frequency $J(0.87\omega_H)$ spectral densities still indicate increased motions in the fast ps–ns timescale compared to most residues in the DED. Nevertheless, fast motions in this region are greatly reduced upon ERK2 binding compared to the free-form, and $J(0.87\omega_H)$ values in this region (residues 121–129) are comparable to at least two residues (E64 and E68) from the DED in the complex form. From the CSP and spectral density results, we believe that residues 121–129 are directly involved in ERK2 binding, consistent with previous observations that a D-site peptide can dissociate PED/PEA-15 from ERK2 complex [13].

The role of the globular DED in ERK2 binding, however, is very complicated. The previous mutagenesis study indicated that D74 is important in binding ERK2, and a single mutation D74A completely abolished the binding capability of PED/PEA-15 [30]. Several other

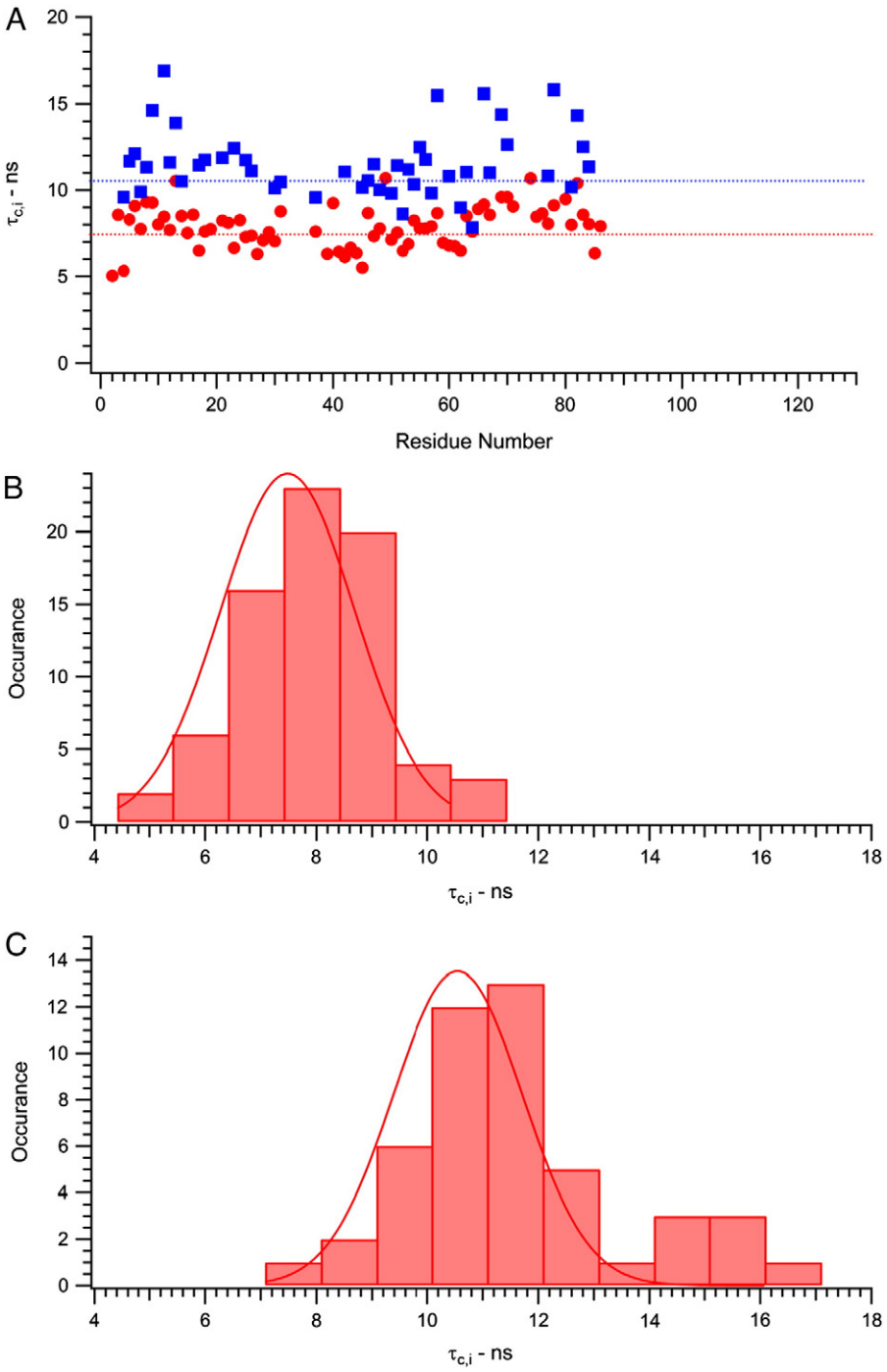

Fig. 4. (A) The per residue correlation times, $\tau_{c,i}$, for rigid DED residues (NOE > 0.7) of PED/PEA-15 in the free (red) and ERK2-bound form. The histograms and Gaussian distributions of $\tau_{c,i}$ for free and ERK2-bound forms are displayed in (B) and (C), respectively. The free-form shows a single distribution centered at 7.5 ns, while the ERK2-bound protein displays a minor distribution at a higher correlation time (~15 ns) in addition to the major distribution centered around 11.5 ns.

residues, including N14, T16, E18, and R71, were also indicated to affect ERK2 binding. These residues are shown on the PED/PEA-15 NMR structure (PDB ID: 1N3K) in Fig. 5A. However, none of these residues stands out in the CSP analysis, and on the contrary, the resonances for these residues experience very little shift upon ERK2 binding (Fig. 1). Interestingly, the HSQC spectra in the original study showed that all of these resonances were broadened out instead of shifted, indicative of intermediate exchange or aggregation. In our TROSY spectra (Fig. 1A), all of these residues are clearly seen in both the free-state and ERK2 complex (labeled in magenta), and their chemical shifts in both dimensions are virtually unchanged. Therefore, the chemical environments surrounding these residues have relatively small variations upon complex formation. The dynamic analyses did not reveal much unusual behavior for these residues in either free- or ERK2-bound form. D74 is part of the charge triad E^{19}-R^{72}xD^{74}L on the DED surface, and we do not expect any major disruption or rearrangement of surface interactions to occur to D74 when PED/PEA-15 binds to ERK2. There are, however, several residues in helices α4 and α5 that experience large CSP, including H52, I63, H65, I66, and I69, and some residues in α5 and α6 have complicated motions as indicated by their higher than average values in both $J(0)$ and $J(0.87\omega_H)$ spectral densities, although none of these residues are

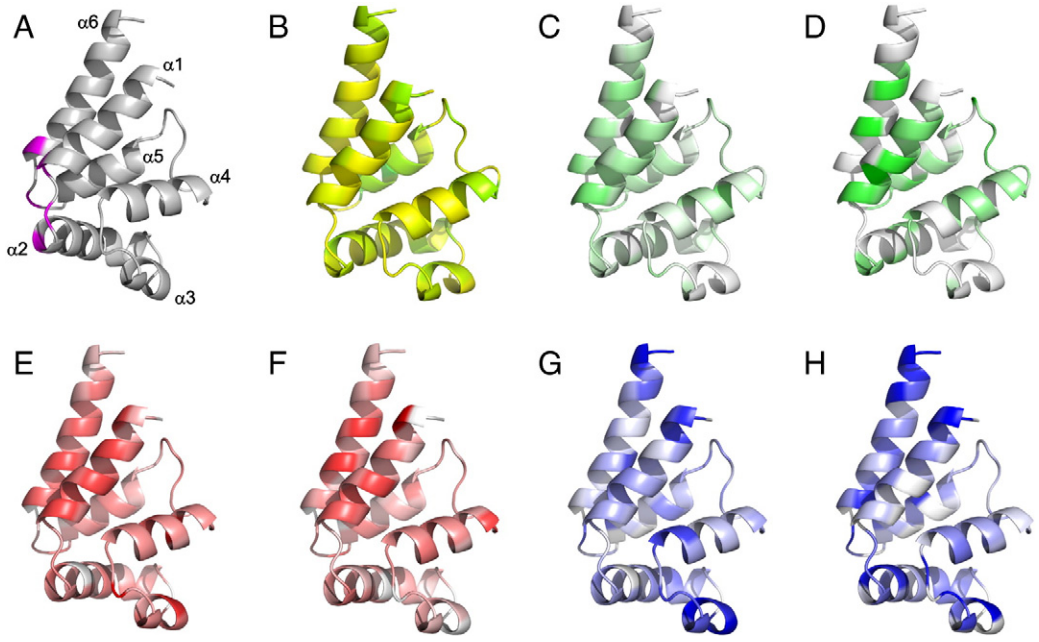

Fig. 5. Molecular structural representations of PED/PEA-15 DED. (A) Residues that are important for ERK2 binding from previous mutagenesis study are colored in magenta. (B) Chemical shift perturbation values are mapped onto the DED structure ramped from bright yellow to dark green as increasing CSP values. The per-residue correlation times for PED/PEA-15 in the free (C) and ERK2-bound forms (D) are mapped onto the DED structure with darker green color represents larger $\tau_{c,i}$ values. Large $\tau_{c,i}$ values (~15 ns) are observed in the helices α1, α5, and α6, suggesting a tight association in this region to ERK2 protein. (E) $J(0)$ and (F) $J(0.87\omega_H)$ values for the PED/PEA-15 in the free form are mapped onto the DED structure with darker red color represents greater values. (G) $J(0)$ and (H) $J(0.87\omega_H)$ values for the PED/PEA-15 in the ERK2-bound form are mapped onto the DED structure with darker blue color represents greater values. The $J(0)$ and $J(0.87\omega_H)$ show opposite trends in general, and residues with darker color in one plot normally show lighter color in the other, although some residues display both increased $J(0)$ and $J(0.87\omega_H)$ values, represented as darker region in both plots. See text for detail.

essential in ERK2 binding from the mutagenesis study. The essential binding residues (N14, T16, E18, R71, D74) are localized on a small surface formed around α1–α2 loop and α5–α6 loop. We speculate that these residues are crucial for binding, not through direct interactions with ERK2, but acting as a hinge and maintaining flexibility of the protein to facilitate the conformational change necessary for binding ERK2. The conformational change, however, does not alter the hinge conformation in any significant way.

We have mapped CSP, $J(0)$, $J(0.87\omega_H)$, and $\tau_{c,i}$ values for DED residues 1–90 onto the NMR structure of PED/PEA-15 (1N3K), together with mapping of residues found to be important in ERK2 binding from the previous mutagenesis study, in Fig. 5. Residues showing large CSP are clustered mostly in helix α5, and most residues with larger CSP values (dark green) are located on the opposite side of the essential residues (Fig. 5B). The per-residue correlation times, $\tau_{c,i}$, are distributed more evenly across the DED in the free-form, with a single distribution center around 8 ns (Fig. 5C), while the ERK2-bound form $\tau_{c,i}$ values are unevenly distributed with two distribution centers at 11 ns and 15 ns. The high $\tau_{c,i}$ values are clustered on the helices α1, α5, and α6 (Fig. 5D), the same locations for residues with high CSP, suggesting a tight association of this region with ERK2. The spectral density functions, $J(0)$ and $J(0.87\omega_H)$, show opposite trends in general, where residues with smaller $J(0)$ densities (lighter color, Fig. 5E and G), have higher $J(0.87\omega_H)$ values (darker color, Fig. 5F and H). Increased $J(0)$ spectral densities are observed for helices α1 and α6, as well as part of α3, for the free PED/PEA-15 (Fig. 5E). Residues with higher than average $J(0.87\omega_H)$ in free PED/PEA-15, indicative of enhanced internal motions in the ps–ns timescale, are located relatively far from the surface location of the essential binding residues (Fig. 5F). Some residues in the middle of helices α1, α3, α5 and α6 show an increase in both $J(0)$ and $J(0.87\omega_H)$ densities, suggesting complicated dynamic behaviors on both fast and slow timescales. Upon complex formation, helices α4 and α5 show increased motions on the μs–ms timescale as indicated by higher than average $J(0)$ spectral densities, while α3 has enhanced motions on the ps–ns timescale reflected in the lower $J(0)$ and larger $J(0.87\omega_H)$ values (Fig. 5G–H). Nevertheless, the spectral density functions do not demonstrate any unusual dynamic characters for the essential binding residues as intermediate $J(0)$ and small $J(0.87\omega_H)$ are observed for the protein in both free- and ERK2-bound form. In either free- or ERK2-bound forms, the most dynamic residues on both slow and fast timescales are mostly located on the opposite side of the surface on which the essential binding residues are found. The dynamic profiles, again, argue strongly that the binding essential residues in PED/PEA-15 are not directly involved in the interactions with ERK2.

Then why are these residues found to highly affect the binding capability of PED/PEA-15 to ERK2? Combining chemical shift perturbation, spectral density analyses and previous results of the mutagenesis study and fluorescence binding assays, we propose the following binding model. Upon recognition of the reversed pseudo D-site sequence, ^{121}IKLAPPPKK^{129}, at the tail of the PED/PEA-15 by the ERK2 D-recruitment site, the essential residues on the DED, through various side-chain interactions (charge–charge, hydrogen bonding, etc.) with other residues on the surface, facilitate conformational change and structural rearrangement of the DED to recognize the ERK2 surface near the F-recruitment site. The PED/PEA-15 uses an induced surface formed from residues on helices α1, α5, and α6 to interact and tumbles together with ERK2, resulting in high $\tau_{c,i}$ values of ~15 ns, while helices α2, α3, α4 are tumbling more freely from ERK2, displaying a lower $\tau_{c,i}$ values of ~11 ns (Fig. 6A). The two tumbling rates are coordinated through the polar interaction network of the charge triad motif, D^{19}-R^{72}xD^{74}L (x = any residue). A single site mutation in the charge triad, D74A, disrupts polar surface interactions on PED/PEA-15, with the resultant loss of the flexibility for conformational rearrangement that is crucial to binding to ERK.

The charge triad is considered a signature feature of the DED, exemplified by the crystal structure of the viral FLICE inhibitory protein MC159 [24,26], and is found in many DED-containing proteins [4]. However, our data does not support any direct contact of the charge triad to the ERK2 binding interface. Interestingly, another ERK2-

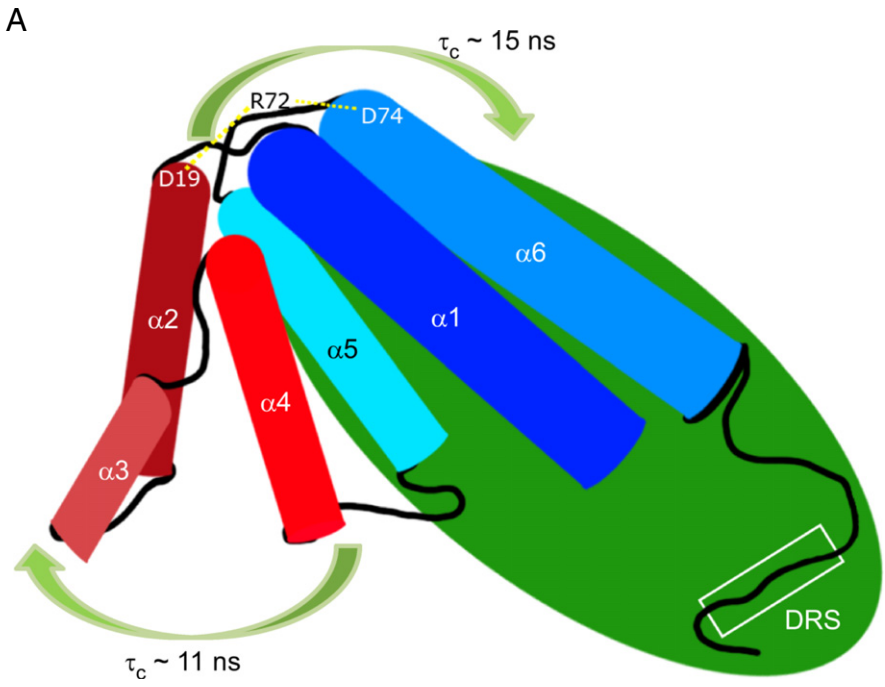

B

```
                                                  ↓  ↓  ↓
PED/PEA-15A DED          1 MAEYGTLLQDLTNNITLEDLEQLKSACKEDIP-SEKSEEITT--GSAWFS   47
Vanishin/PEA-15B DED    29 TSEYRTLLQDRQHHS--LRQGQLKSACKEEIP-SEKTEEITA--GSAWVS   73

                                                        ↓     ↓
PED/PEA-15A DED         48 FLESHNKLDKD-NLSYIEHIFEISRRPDLLTMVVDYRTRVLKIS        90
Vanishin/PEA-15B DED    74 FLESHNTLHQDSTVSYTEHVFEISHCHDLLGMMVNLCAEDLRTG       117
```

Fig. 6. (A) Interaction model of PED/PEA-15 and ERK2. The C-terminal tail containing the reversed pseudo D-site sequence binds to the D-recruitment site on ERK2. Conformational changes on PED/PEA-15 DED expose binding surface on the helices α1, α5, and α6 that interact and tumble with ERK2 at a high correlation time (~15.1 ns), while helices α2, α3, and α4 are tumbling relatively freely from the ERK2 at a lower correlation time (~11 ns). The charge triad motif, D19-R72-D74, coordinates the conformational change by maintaining the orientations of the side chains. (B) Sequence alignment of death effector domains of PED/PEA-15 and vanishin/PEA-15b. The conserved charge triad D/E-RxDL residues are colored in dark blue, conserved hydrophobic residues in magenta, charged residues in cyan, and polar, uncharged residues in green. PED/PEA-15 residues important in ERK2 binding identified from a mutagenesis study are indicated by small arrows on top of the sequence. The nuclear exporting sequence (NES) of PED/PEA-15 is underlined in the sequence.

binding protein, vanishin/PEA-15b, whose sequence is highly homologous to PED/PEA-15 protein with 77% similarity over 81 DED residues [50], lacks the first two residues in the charge triad motif (Fig. 6B). This also supports the argument that the charge triad is not directly involved in ERK2 binding. In addition, besides ERK2 binding, vanishin/PEA-15b does not seem to bind other DED-containing proteins [50], suggesting that the charge triad might be essential in DED–DED interactions, but might not be directly involved in ERK2 complex formation. The vanishin/PEA-15b protein sequence differs from PED/PEA-15 mostly in the first 20 amino acids in the DED, where PED/PEA-15 contains a nuclear exporting sequence (NES), underlined in Fig. 6B. The NES on PED/PEA-15 promotes nuclear export of ERK to the cytoplasm. Vanishin/PEA-15b does not appear to have an NES anywhere in its sequence, and it accumulates predominantly in the nucleus and the Golgi [50]. Several residues important in ERK2 binding are found in the vicinity of the NES on PED/PEA-15, including N14, T16, and E18. Therefore, these residues may have different roles in the binding with ERK2. Another major difference between PED/PEA-15 and vanishin/PEA-15b is the role of the unstructured tail in ERK2 binding. The previous mutagenesis study [30], fluorescence binding assay [13], and our current CSP and dynamic analyses, all point to the essential roles of the C-terminal tail of PED/PEA-15, and minor changes in the tail will disrupt ERK2 binding completely. Vanishin/PEA-15b protein has its DED in the middle of the sequence, with a 28-residue N-terminal tail and a 10-residue C-terminal tail. However, no sequence similarity to the PED/PEA-15 tail or D/F-site sequence can be found on either side of the DED in vanishin/PEA-15b. It is not clear if the N- or C-terminal tails of vanishin/PEA-15b are important in ERK2 binding, but it suggests that vanishin/PEA-15b protein might bind to ERK2 in a completely different manner.

The complex dynamic behaviors observed for PED/PEA-15 in both free- and ERK2-bound forms, in our opinion, match very well with its multifunctional roles in regulating various fundamental cellular processes in apoptosis, ERK/MAP kinase pathway, and glucose metabolism. For a small, non-catalytic, protein like PED/PEA-15 to perform multiple functions in remotely related processes, the protein must be able to maximize the available binding interface to interact with different targets. Besides ERK2 binding, which requires residues from both the DED and the C-terminal tails, PED/PEA-15 interacts with other DED-containing proteins, such as FADD and procaspase-8, putatively through one of the canonical death domain superfamily interfaces as illustrated in the crystal structure of a death domain assembly [23], while it utilizes its first 24 residues to interact with phospholipase D1 [51]. In addition to available binding interfaces, the protein should also maintain a wide range of dynamics in order to adapt to its binding partners (induced fit), which have distinctly different shapes and properties. In terms of ERK binding, PED/PEA-15 binds to activated ERK, preventing ERK protein from relocating into the nucleus from the cytoplasm, a dynamically complicated process. Therefore, we believe that the dynamic complexity

of PED/PEA-15 contributes to its functional flexibility in regulating unrelated physiological processes throughout the body.

Acknowledgement

We thank Dr. Justine Hill and Yu Wei for cloning, expression, and labeling of PED/PEA-15 and ERK2. We thank the New York Structural Biology Center for 800 MHz NMR instrument time. We are also grateful for various funding and fellowships from the Celgene Corporation, Eric F. Ross Research Fellowship, New Jersey Space Grant Consortium/NASA, and the Reverend Owen Garrigan Endowed Memorial Scholarship.

Appendix A. Supplementary data

Supplementary data to this article can be found online at http://dx.doi.org/10.1016/j.bbapap.2012.07.001.

References

[1] N. Danziger, M. Yokoyama, T. Jay, J. Cordier, J. Glowinski, H. Chneiweiss, Cellular expression, developmental regulation, and phylogenic conservation of PEA-15, the astrocytic major phosphoprotein and protein kinase C substrate, J. Neurochem. 64 (1995) 1016–1025.
[2] A. Estellés, M. Yokoyama, F. Nothias, J.-D. Vincent, J. Glowinski, P. Vernier, H. Chneiweiss, The major astrocytic phosphoprotein PEA-15 is encoded by two mRNAs conserved on their full length in mouse and human, J. Biol. Chem. 271 (1996) 14800–14806.
[3] M. Valmiki, J. Ramos, Death effector domain-containing proteins, Cell. Mol. Life Sci. 66 (2009) 814–830.
[4] H.H. Park, Y.-C. Lo, S.-C. Lin, L. Wang, J.K. Yang, H. Wu, The death domain superfamily in intracellular signaling of apoptosis and inflammation, Annu. Rev. Immunol. 25 (2007) 561–586.
[5] H. Renganathan, H. Vaidyanathan, A. Knapinska, J.W. Ramos, Phosphorylation of PEA-15 switches its binding specificity from ERK/MAPK to FADD, Biochem. J. 390 (2005) 729–735.
[6] J. Krueger, F.-L. Chou, A. Glading, E. Schaefer, M.H. Ginsberg, Phosphorylation of phosphoprotein enriched in astrocytes (PEA-15) regulates extracellular signal-regulated kinase-dependent transcription and cell proliferation, Mol. Biol. Cell 16 (2005) 3552–3561.
[7] H. Araujo, N. Danziger, J. Cordier, J. Glowinski, H. Chneiweiss, Characterization of PEA-15, a major substrate for protein kinase C in astrocytes, J. Biol. Chem. 268 (1993) 5911–5920.
[8] M. Kubes, J. Cordier, J. Glowinski, J.-A. Girault, H. Chneiweiss, Endothelin induces a calcium-dependent phosphorylation of PEA-15 in intact astrocytes: identification of Ser104 and Ser116 phosphorylated, respectively, by protein kinase C and calcium/calmodulin kinase II in vitro, J. Neurochem. 71 (1998) 1307–1314.
[9] A. Trencia, A. Perfetti, A. Cassese, G. Vigliotta, C. Miele, F. Oriente, S. Santopietro, F. Giacco, G. Condorelli, P. Formisano, F. Beguinot, Protein kinase B/Akt binds and phosphorylates PED/PEA-15, stabilizing its antiapoptotic action, Mol. Cell. Biol. 23 (2003) 4511–4521.
[10] D. Kitsberg, E. Formstecher, M. Fauquet, M. Kubes, J. Cordier, B. Canton, G. Pan, M. Rolli, J. Glowinski, H. Chneiweiss, Knock-out of the neural death effector domain protein PEA-15 demonstrates that its expression protects astrocytes from TNFα-induced apoptosis, J. Neurosci. 19 (1999) 8244–8251.
[11] C. Xiao, B.F. Yang, N. Asadi, F. Beguinot, C. Hao, Tumor necrosis factor-related apoptosis-inducing ligand-induced death-inducing signaling complex and its modulation by c-FLIP and PED/PEA-15 in glioma cells, J. Biol. Chem. 277 (2002) 25020–25025.
[12] E. Formstecher, J.W. Ramos, M. Fauquet, D.A. Calderwood, J.-C. Hsieh, B. Canton, X.-T. Nguyen, J.-V. Barnier, J. Camonis, M.H. Ginsberg, H. Chneiweiss, PEA-15 mediates cytoplasmic sequestration of ERK MAP kinase, Dev. Cell 1 (2001) 239–250.
[13] K. Callaway, O. Abramczyk, L. Martin, K.N. Dalby, The anti-apoptotic protein PEA-15 is a tight binding inhibitor of ERK1 and ERK2, which blocks docking interactions at the d-recruitment site, Biochemistry 46 (2007) 9187–9198.
[14] G. Condorelli, G. Vigliotta, A. Cafieri, A. Trencia, P. Andalo, F. Oriente, C. Miele, M. Caruso, P. Formisano, F. Beguinot, PED/PEA-15: an anti-apoptotic molecule that regulates FAS/TNFR1-induced apoptosis, Oncogene 18 (1999) 4409–4415.
[15] Y. Zhang, O. Redina, Y.M. Altshuller, M. Yamazaki, J. Ramos, H. Chneiweiss, Y. Kanaho, M.A. Frohman, Regulation of expression of phospholipase D1 and D2 by PEA-15, a novel protein that interacts with them, J. Biol. Chem. 275 (2000) 35224–35232.
[16] G. Condorelli, G. Vigliotta, C. Iavarone, M. Caruso, C.G. Tocchetti, F. Andreozzi, A. Cafieri, M.F. Tecce, P. Formisano, L. Beguinot, F. Beguinot, PED/PEA-15 gene controls glucose transport and is overexpressed in type 2 diabetes mellitus, EMBO J. 17 (1998) 3858–3866.
[17] G. Vigliotta, C. Miele, S. Santopietro, G. Portella, A. Perfetti, M.A. Maitan, A. Cassese, F. Oriente, A. Trencia, F. Fiory, C. Romano, C. Tiveron, L. Tatangelo, G. Troncone, P. Formisano, F. Beguinot, Overexpression of the ped/pea-15 gene causes diabetes by impairing glucose-stimulated insulin secretion in addition to insulin action, Mol. Cell. Biol. 24 (2004) 5005–5015.
[18] C. Cruz, F. Cruz, The ERK 1 and 2 pathway in the nervous system: from basic aspects to possible clinical applications in pain and visceral dysfunction, Curr. Neuropharmacol. 5 (2007) 244–252.
[19] Z. Chen, T.B. Gibson, F. Robinson, L. Silvestro, G. Pearson, B.-E. Xu, A. Wright, C. Vanderbilt, M.H. Cobb, MAP kinases, Chem. Rev. 101 (2001) 2449–2476.
[20] T.S. Lewis, P.S. Shapiro, N.G. Ahn, Signal transduction through MAP kinase cascades, In: in: F.V.W. George, K. George (Eds.), Advances in Cancer Research, volume 74, Academic Press, 1998, pp. 49–139.
[21] P. Formisano, G. Perruolo, S. Libertini, S. Santopietro, G. Troncone, G.A. Raciti, F. Oriente, G. Portella, C. Miele, F. Beguinot, Raised expression of the antiapoptotic protein ped//pea-15 increases susceptibility to chemically induced skin tumor development, Oncogene 24 (2005) 7012–7021.
[22] L. Wang, J.K. Yang, V. Kabaleeswaran, A.J. Rice, A.C. Cruz, A.Y. Park, Q. Yin, E. Damko, S.B. Jang, S. Raunser, C.V. Robinson, R.M. Siegel, T. Walz, H. Wu, The Fas-FADD death domain complex structure reveals the basis of DISC assembly and disease mutations, Nat. Struct. Mol. Biol. 17 (2010) 1324–1329.
[23] H.H. Park, E. Logette, S. Raunser, S. Cuenin, T. Walz, J. Tschopp, H. Wu, Death domain assembly mechanism revealed by crystal structure of the oligomeric PIDDosome core complex, Cell 128 (2007) 533–546.
[24] J.K. Yang, L. Wang, L. Zheng, F. Wan, M. Ahmed, M.J. Lenardo, H. Wu, Crystal structure of MC159 reveals molecular mechanism of DISC assembly and FLIP inhibition, Mol. Cell 20 (2005) 939–949.
[25] M.-F. Gaumont-Leclerc, U.K. Mukhopadhyay, S. Goumard, G. Ferbeyre, PEA-15 is inhibited by adenovirus E1A and plays a role in ERK nuclear export and Ras-induced senescence, J. Biol. Chem. 279 (2004) 46802–46809.
[26] F.-Y. Li, P.D. Jeffrey, J.W. Yu, Y. Shi, Crystal structure of a viral FLIP, J. Biol. Chem. 281 (2006) 2960–2968.
[27] C. Bartholomeusz, H. Itamochi, M. Nitta, H. Saya, M.H. Ginsberg, N.T. Ueno, Antitumor effect of E1A in ovarian cancer by cytoplasmic sequestration of activated ERK by PEA15, Oncogene 25 (2005) 79–90.
[28] C. Bartholomeusz, A.M. Gonzalez-Angulo, A. Kazansky, S. Krishnamurthy, P. Liu, L.X.H. Yuan, F. Yamasaki, S. Liu, N. Hayashi, D. Zhang, F.J. Esteva, G.N. Hortobagyi, N.T. Ueno, PEA-15 inhibits tumorigenesis in an MDA-MB-468 triple-negative breast cancer xenograft model through increased cytoplasmic localization of activated extracellular signal-regulated kinase, Clin. Cancer Res. 16 (2010) 1802–1811.
[29] C. Bartholomeusz, D. Rosen, C. Wei, A. Kazansky, F. Yamasaki, T. Takahashi, H. Itamochi, S. Kondo, J. Liu, N.T. Ueno, PEA-15 induces autophagy in human ovarian cancer cells and is associated with prolonged overall survival, Cancer Res. 68 (2008) 9302–9310.
[30] J.M. Hill, H. Vaidyanathan, J.W. Ramos, M.H. Ginsberg, M.H. Werner, Recognition of ERK MAP kinase by PEA-15 reveals a common docking site within the death domain and death effector domain, EMBO J. 21 (2002) 6494–6504.
[31] B. Farina, L. Pirone, L. Russo, F. Viparelli, N. Doti, C. Pedone, E.M. Pedone, R. Fattorusso, NMR backbone dynamics studies of human PED/PEA-15 outline protein functional sites, FEBS J. 277 (2010) 4229–4240.
[32] K. Callaway, M.A. Rainey, K.N. Dalby, Quantifying ERK2–protein interactions by fluorescence anisotropy: PEA-15 inhibits ERK2 by blocking the binding of DEJL domains, Biochim. Biophys. Acta—Prot Proteomics 1754 (2005) 316–323.
[33] T.S. Kaoud, A.K. Devkota, R. Harris, M.S. Rana, O. Abramczyk, M. Warthaka, S. Lee, M.E. Girvin, A.F. Riggs, K.N. Dalby, Activated ERK2 is a monomer in vitro with or without divalent cations and when complexed to the cytoplasmic scaffold PEA-15, Biochemistry 50 (2011) 4568–4578.
[34] F. Zhang, D.J. Robbins, M.H. Cobb, E.J. Goldsmith, Crystallization and preliminary X-ray studies of extracellular signal-regulated kinase-2/MAP kinase with an incorporated His-tag, J. Mol. Biol. 233 (1993) 550–552.
[35] K. Pervushin, R. Riek, G. Wider, K. Wüthrich, Attenuated T2 relaxation by mutual cancellation of dipole–dipole coupling and chemical shift anisotropy indicates an avenue to NMR structures of very large biological macromolecules in solution, Proc. Natl. Acad. Sci. U. S. A. 94 (1997) 12366–12371.
[36] K. Pervushin, Impact of Transverse Relaxation Optimized Spectroscopy (TROSY) on NMR as a technique in structural biology, Q. Rev. Biophys. 33 (2001) 161–197.
[37] G. Zhu, Y. Xia, L.K. Nicholson, K.H. Sze, Protein dynamics measurements by TROSY-based NMR experiments, J. Magn. Reson. 143 (2000) 423–426.
[38] F. Delaglio, S. Grzesiek, G.W. Vuister, G. Zhu, J. Pfeifer, A. Bax, NMRPipe: a multidimensional spectral processing system based on UNIX pipes, J. Biomol. NMR 6 (1995) 277–293.
[39] B.A. Johnson, R.A. Blevins, NMR View: a computer program for the visualization and analysis of NMR data, J. Biomol. NMR 4 (1994) 603–614.
[40] L. Spyracopoulos, A suite of Mathematica notebooks for the analysis of protein main chain 15N NMR relaxation data, J. Biomol. NMR 36 (2006) 215–224.
[41] N.A. Farrow, O. Zhang, J.D. Forman-Kay, L.E. Kay, Comparison of the backbone dynamics of a folded and an unfolded SH3 domain existing in equilibrium in aqueous buffer, Biochemistry 34 (1995) 868–878.
[42] N.A. Farrow, O. Zhang, J.D. Forman-Kay, L.E. Kay, Characterization of the backbone dynamics of folded and denatured states of an SH3 domain, Biochemistry 36 (1997) 2390–2402.
[43] J.H. Viles, D. Donne, G. Kroon, S.B. Prusiner, F.E. Cohen, H.J. Dyson, P.E. Wright, Local structural plasticity of the prion protein. Analysis of NMR relaxation dynamics, Biochemistry 40 (2001) 2743–2753.
[44] A.G. Palmer, M. Rance, P.E. Wright, Intramolecular motions of a zinc finger DNA-binding domain from Xfin characterized by proton-detected natural abundance carbon-13 heteronuclear NMR spectroscopy, J. Am. Chem. Soc. 113 (1991) 4371–4380.

[45] A.M. Mandel, M. Akke, I.I.I.A.G. Palmer, Backbone dynamics of *Escherichia coli* ribonuclease HI: correlations with structure and function in an active enzyme, J. Mol. Biol. 246 (1995) 144–163.
[46] R. Cole, J.P. Loria, FAST-Modelfree: a program for rapid automated analysis of solution NMR spin-relaxation data, J. Biomol. NMR 26 (2003) 203–213.
[47] P. Dosset, J.-C. Hus, M. Blackledge, D. Marion, Efficient analysis of macromolecular rotational diffusion from heteronuclear relaxation data, J. Biomol. NMR 16 (2000) 23–28.
[48] J.W. Peng, G. Wagner, Frequency spectrum of NH bonds in Eglin c from spectral density mapping at multiple fields, Biochemistry 34 (1995) 16733–16752.
[49] C. Bracken, P.A. Carr, J. Cavanagh, A.G. Palmer Iii, Temperature dependence of intramolecular dynamics of the basic leucine zipper of GCN4: implications for the entropy of association with DNA, J. Mol. Biol. 285 (1999) 2133–2146.
[50] R. Sur, J.W. Ramos, Vanishin is a novel ubiquitinylated death-effector domain protein that blocks ERK activation, Biochem. J. 387 (2005) 315–324.
[51] F. Viparelli, A. Cassese, N. Doti, F. Paturzo, D. Marasco, N.A. Dathan, S.M. Monti, G. Basile, P. Ungaro, M. Sabatella, C. Miele, R. Teperino, E. Consiglio, C. Pedone, F. Beguinot, P. Formisano, M. Ruvo, Targeting of PED/PEA-15 molecular interaction with phospholipase D1 enhances insulin sensitivity in skeletal muscle cells, J. Biol. Chem. 283 (2008) 21769–21778.